Resource

Chemistry & Biology

Structuring Microbial Metabolic Responses to Multiplexed Stimuli via Self-Organizing Metabolomics Maps

Graphical Abstract

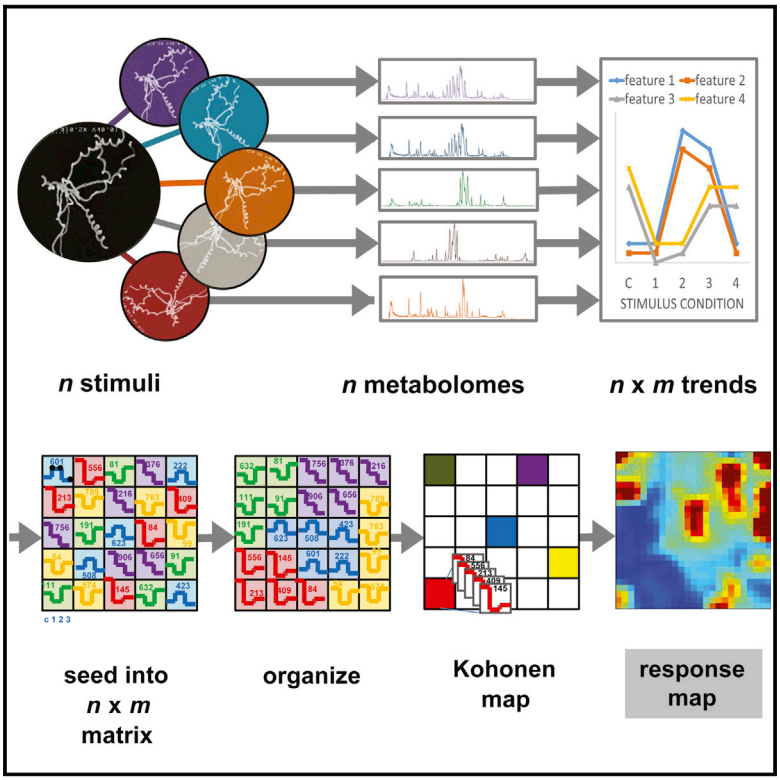

Authors

Cody R. Goodwin, Brett C. Covington, ..., John A. McLean, Brian O. Bachmann

Correspondence

brian.bachmann@vanderbilt.edu (B.O.B.), john.a.mclean@vanderbilt.edu (J.A.M.)

In Brief

Microbial genome sequencing reveals a large untapped potential for the discovery of new natural products drugs from microorganisms. Here Goodwin et al. use a combination of discrete chemical and biological stimuli and a big data approach to stimulate and identify natural products in a model organism producer.

Highlights

- Secondary metabolite expression is triggered by environmental stimuli
- Using stimuli and self-organizing maps, we identify a response metabolome
- Mapping responses to multiplexed stimuli reveal secondary metabolites
- In *S. coelicolor*, this revealed a large fraction of its biosynthetic potential

Goodwin et al., 2015, Chemistry & Biology *22*, 661–670
May 21, 2015
http://dx.doi.org/10.1016/j.chembiol.2015.03.020

CellPress

Chemistry & Biology
Resource

Structuring Microbial Metabolic Responses to Multiplexed Stimuli via Self-Organizing Metabolomics Maps

Cody R. Goodwin,[1,2,5] Brett C. Covington,[1] Dagmara K. Derewacz,[1] C. Ruth McNees,[1] John P. Wikswo,[2,4] John A. McLean,[1,2,3,5,*] and Brian O. Bachmann[1,2,3,*]
[1]Department of Chemistry, Vanderbilt University, 7300 Stevenson Center, Nashville, TN 37235, USA
[2]Vanderbilt Institute for Integrative Biosystems Research and Education, Vanderbilt University, 6301 Stevenson Center, Nashville, TN 37235, USA
[3]Vanderbilt Institute of Chemical Biology, Vanderbilt University, 7300 Stevenson Center, Nashville, TN 37235, USA
[4]Department of Biomedical Engineering, Department of Molecular Physiology and Biophysics, and Department of Physics and Astronomy, Vanderbilt University, 6301 Stevenson Center, Nashville, TN 37235, USA
[5]Center for Innovative Technology, Vanderbilt University, 5401 Stevenson Center, Nashville, TN 37235, USA
*Correspondence: brian.bachmann@vanderbilt.edu (B.O.B.), john.a.mclean@vanderbilt.edu (J.A.M.)
http://dx.doi.org/10.1016/j.chembiol.2015.03.020

SUMMARY

Secondary metabolite biosynthesis in microorganisms responds to discrete chemical and biological stimuli; however, untargeted identification of these responses presents a significant challenge. Herein we apply multiplexed stimuli to *Streptomyces coelicolor* and collect the resulting response metabolomes via ion mobility-mass spectrometric analysis. Self-organizing map (SOM) analytics adapted for metabolomic data demonstrate efficient characterization of the subsets of primary and secondary metabolites that respond similarly across stimuli. Over 60% of all metabolic features inventoried from responses are either not observed under control conditions or produced at greater than 2-fold increase in abundance in response to at least one of the multiplexing conditions, reflecting how metabolites encode phenotypic changes in an organism responding to multiplexed challenges. Using abundance as an additional filter, each of 16 known *S. coelicolor* secondary metabolites is prioritized via SOM and observed at increased levels (1.2- to 22-fold compared with unperturbed) in response to one or more challenge conditions.

INTRODUCTION

Microbial producers of secondary metabolites typically contain gene clusters encoding dozens of secondary metabolite families (Zerikly and Challis, 2009), the expression of which appears to be tightly regulated in response to discrete chemical and/or biological stimulus. For example, exposure of actinomycetes to mixed fermentation conditions has demonstrated that secondary metabolite families are produced selectively via intergeneric (Onaka et al., 2011; Traxler et al., 2013) and interkingdom (Moree et al., 2012) microbial interactions. Similarly, the acquisition of antibiotic resistance via point mutations (Hosaka et al., 2009; Tanaka et al., 2013), exposure to rare earth metals (Tanaka et al., 2010; Ochi et al., 2014), exposure to small molecules (Craney et al., 2012; Seyedsayamdost, 2014), and the formulation of production media (Bode et al., 2002) have also been linked to gene-cluster-specific upregulation of secondary metabolites in actinomycetes. These data are consistent with secondary metabolites governing adaptive organismal responses to environmental stimuli. Identifying secondary metabolites and associating them to gene clusters that are linked to discrete chemical and biological stimuli can provide insight into the chemical ecological role of secondary metabolites. Moreover, the ability to selectively stimulate native expression of secondary metabolic gene clusters via chemical or biological stimuli and detect their corresponding products without resorting to genetic recombinant methods would greatly expedite microbial secondary metabolite discovery.

If secondary and primary metabolite regulation has adapted to selectively respond to chemical and biological stimuli, then metabolites possessing selective responses may be identifiable within metabolomes by possessing characteristic abundance trends across multiplexed stimulus conditions. To investigate this hypothesis and enable secondary metabolite discovery, we herein assess the potential for stimulus-mediated production of secondary metabolites in the native microbe by multiplexed chemical and biological stimulation. To access a broad spectrum of responses, a battery of 23 perturbations in a single growth medium was utilized from three reported categories of activating conditions for *Streptomyces coelicolor A3(2)*. The resulting collected sum of detectable metabolomic response inventories was analyzed by ultra-performance liquid chromatography-ion mobility-mass spectrometric (UPLC-IM-MS) analysis. To structure and categorize the response specificity of metabolic features within these data, we developed and implemented a self-organizing map (SOM)-based analysis (Goodwin et al., 2014; Eichler et al., 2003) for the identification and prioritization of increased metabolite production resulting from the multiplexed perturbations. SOM analysis converted the collected metabolomes into a navigable topological response phenotype map and efficiently identified specific primary and secondary

metabolites that are produced at increased levels in response to stimuli. For example, in primary metabolism, we identified discrete changes in guanosine and phenylalanine pools on lanthanide exposure and evidence of unique adaptive cell wall remodeling in several conditions. Notably, a large fraction (16 total secondary metabolites) of detected secondary metabolites was prioritized via this workflow as the most intense response-specific features, providing insight into the roles that secondary metabolism play in adapting to chemical stimuli and microbial interactions. The combination of multiplexed stimulation of native expression and structuring of the resulting metabolomic responses comprise a generalizable method for activating and detecting products of natively regulated primary and secondary metabolism.

RESULTS

Multiplexing Stimuli of Secondary Metabolism

S. coelicolor A3(2) was cultivated under a battery of processes known to potentiate secondary metabolism. *S. coelicolor* was selected as a model microorganism because it has been extensively mined for secondary metabolites (Bentley et al., 2002), methods for native gene cluster activation have been most commonly developed for this organism (Hosaka et al., 2009; Luti and Mavituna, 2011; Tanaka et al., 2010; Xu et al., 2002), and the majority of secondary metabolites isolated from this strain have been correlated to a gene cluster (Barona-Gomez et al., 2006; Bentley et al., 2002; Challis, 2013; Song et al., 2006).

We selected three known categories of activating stimuli: eliciting spontaneous resistance to transcription or translation-targeting antibiotics, exposure to rare earth elements, and cultivation in the presence of competing microorganisms. Our specific adaptations and standardizations of these reported methods are described in the Supplemental Information. In brief, using a single growth medium (International Streptomyces Protocol 2, ISP2), we cultivated (1) liquid cultures in the presence and absence of five separate scandium or five lanthanum concentrations, (2) liquid cultures of ten different spontaneous rifampicin- or streptomycin-resistance mutants, and (3) agar plate ISP2 co-cultures with three different challenge organisms, *Micrococcus luteus*, *Rhodococcus wratislaviensis*, or *Tsukamurella pulmonis*. Hence, we generated a total of 23 conditions, including controls, spanning these three methodologies.

Total cellular extracts were generated from fermentations via methanol extraction, concentrated, and processed for reverse phase UPLC analysis. Technical triplicates of extracts were analyzed in a randomized sequence using UPLC-IM-MS (Waters Synapt G2) with lock mass correction to provide accurate mass measurements. During each spectral acquisition, an intact and fragmentation spectrum was taken for all ions present (herein referred to as MS^E analysis (Plumb et al., 2006; Goodwin et al., 2012; McLean, 2009). Fragmentation was performed subsequent to IM separation, which allowed for the correlation of product ions to precursor origins through matched mobility.

Raw data were converted to distinct mass-to-charge (m/z) and retention time (R_t) pairs, termed features, and aligned across all samples (Smith et al., 2006). The resultant data matrix of discrete features, or ions, and associated intensities for each condition were averaged across technical replicates and subjected to multivariate statistical analysis (MVSA) and SOM.

Identifying Products of Multiplexed Stimulation through MVSA

The identification of new metabolites with characteristic responses from multiplexed microbial stimuli requires methods for comparing and classifying co-varying ions in the response inventories. Recently, we (Derewacz et al., 2013) and others (Hou et al., 2012; Robinette et al., 2012) have presented MVSA approaches for identifying the most abundant new ions resulting from individual stimulating microbial metabolic perturbations. MVSA methods for data analysis are powerful tools for identifying distinguishing features of small datasets (2–3 conditions) or extracting information regarding global sample grouping, and which metabolites contribute to coarse trends. However, MVSA methods are not ideal for similar prioritization of metabolites in multiplexed perturbations as MVSA is inherently biased for the largest differences among perturbations and is limited in the ability to reflect multiple stimuli in two- or three-dimensional space. Therefore, it omits the lower abundance or minorly co-varying, yet still unique, metabolic reflexes (i.e., changes in metabolism resulting from a stimulus). In applying our previously described MSVA workflow (Derewacz et al., 2013) to the 23 conditions, as shown in Figure 1A, we can visualize the gross distinctions of metabolomic profiles that exist among different stimuli. When each perturbation is analyzed in isolation (Figures 1B–1D), the distinct differences in global metabolism shifts are seen. A loadings plot analysis can be used to determine which ions contribute to sample distinction, as seen in Figure S3A. For comparison, detected secondary metabolites are annotated, which highlights a significant shortcoming of MVSA-based prioritization for a large number of culturing conditions; the largest contributors to sample differences are highlighted but specific features of interest can be masked by the covariance of many species in the dataset. To garner conditionally distinct differences, experimental subsets (see Figures 1B–1D), or even smaller subsets (e.g., a single co-culture versus monocultures or orthogonal partial least squares-discriminant analysis approaches) can be analyzed. Thus, MVSA is most suitable for the interrogation of small datasets where the number of species is low (e.g., <50). However, for 25 conditions, pairwise analysis of multiple iterations of stimulus conditions for prioritization purposes becomes a time-intensive method of prioritizing secondary metabolites from extracts. As a result, we have developed and applied SOM-based methods to ion association and filtering. The primary advantage of SOM-based methods is that they are not prone to masking low-abundant species of interest in the comparison of large datasets (e.g., >50).

Identifying Products of Multiplexed Stimulation by Self-Organizing Maps

Assessing trends in a large number of biochemical or biological conditions requires methods for the rapid visualization and organization of distinct differences in metabolic profiles across many perturbations to sort ions in a response-dependent manner. To address this, we developed a SOM-based approach to sort the complete inventory of ions across all growth conditions into regions based upon similarities in abundance profiles across

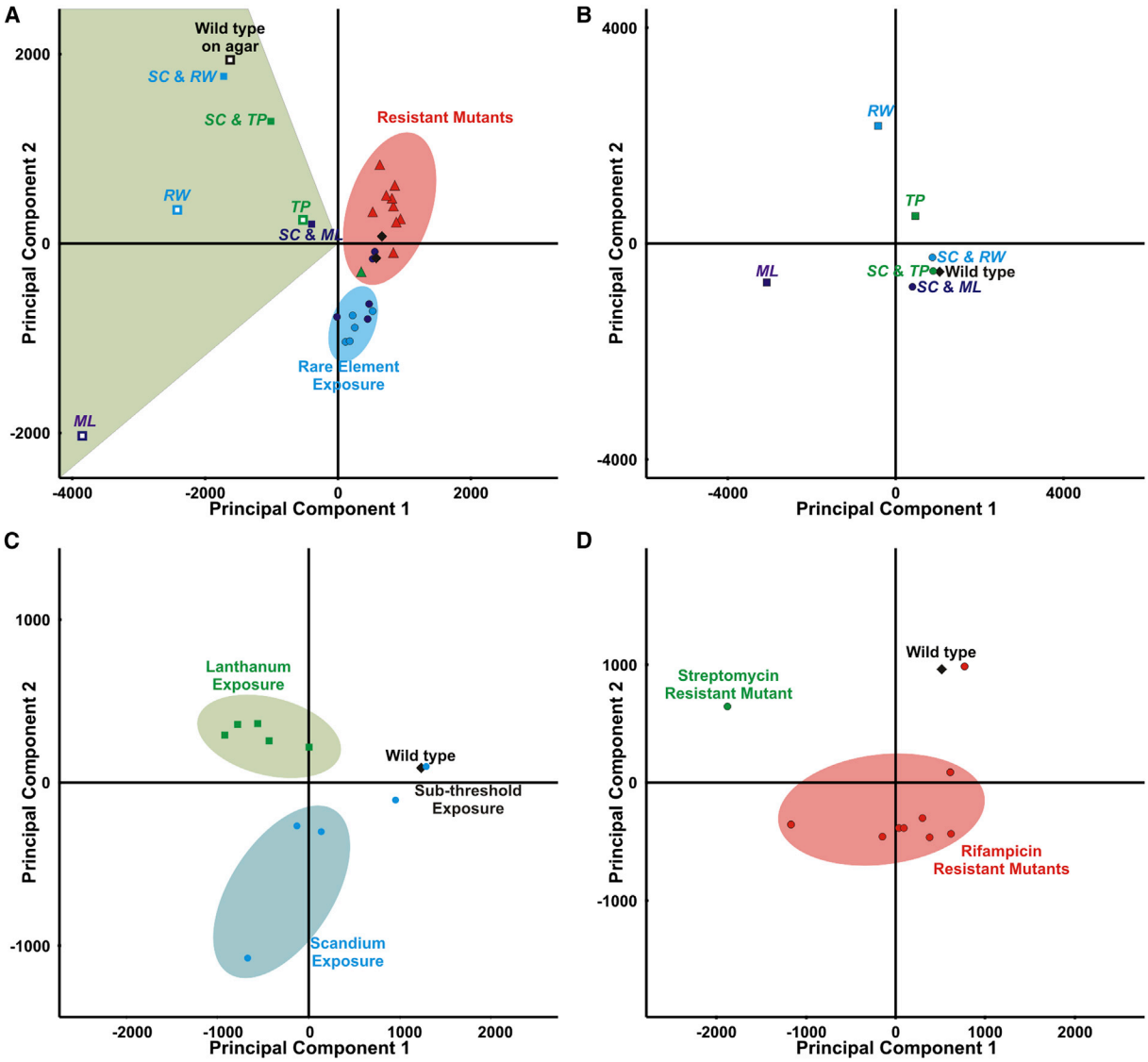

Figure 1. Principal Component Analyses of Metabolomic Inventories

(A) PCA of all cultures.

(B) Co-culture of *S. coelicolor* (SC) with *M. luteus* (ML), *R. wratislaviensis* (RW), and *T. pulmonis* (TP).

(C) Metabolomic profiles in response to rare earth metals.

(D) Comparison of antibiotic-resistant mutants selected by plating on rifampicin and streptomycin.

experiments. This method is particularly well suited for secondary metabolite prioritization, as secondary metabolites are the end products of biochemical pathways and accumulate during fermentation. Differentially expressed, high abundance ions may be ranked subsequent to SOM analysis using the percent contribution of an ion to a region of interest (ROI) on the self-organized map. These ROIs exclusively contain features that respond specifically to a particular perturbation, while other loosely regulated metabolites will cluster outside these prioritized regions. This method then prioritizes metabolites in a response-specific manner that performs well for the comparison of large datasets. Note that, statistically, MVSA and SOM perform similar comparisons but represent the resulting comparisons in a different graphical manner. In fact, many SOM approaches approximate a similar graphical presentation to MVSA when the datasets decrease to a small number of comparisons (ca. 10–50). Thus, the choice of one approach versus the other directly depends on how a specific query is framed and the corresponding number of features to be compared across datasets.

Figure 2 demonstrates the general workflow of the SOM-based approach as applied to multiple perturbing conditions. Experimental and control conditions are processed by UPLC-IM-MS (step 1), significant *m/z* retention time features are identified, and integrated intensity trends lines are generated for each feature. SOM analysis of these feature trends is performed

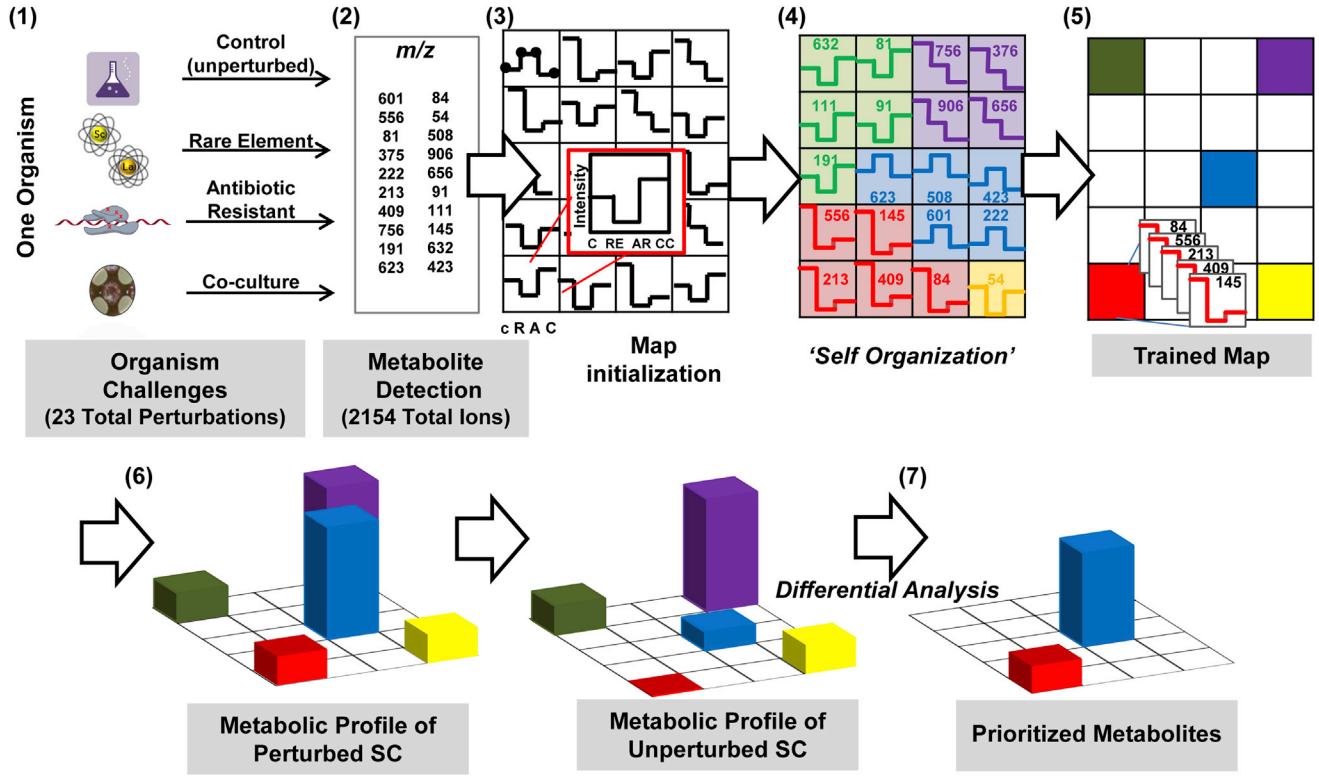

Figure 2. The General Self-Organizing Map-Based Approach to Feature Prioritization

(1) This method begins with extracts from cultures of an organism cultivated under a battery of perturbing conditions. (2) Extracts are analyzed using UPLC-IM-MSE (or other feature-producing methodology) and converted into a matrix of discrete, aligned peaks with associated intensities for each culturing condition. (3–5) These features are then organized based upon intensity trends across culturing conditions. (6) Subsequently, extracts are represented as heat maps based upon the sum abundance of each organized metabolite in a region. (7) Differential analysis comparing data from perturbed cultures with controls allows generation of regions of interest.

using the Gene Expression Dynamics Investigator (GEDI) software (step 2) (Eichler et al., 2003). For a more in-depth description, see Figure S2. Conceptually, detected ion abundance trends are first randomly seeded into a user-defined asymmetric grid (step 3). The coordinates of the grid are only meaningful in relation to other grid locations and have no associated dimensions. Feature intensity trends are then iteratively organized based upon intensity similarities across experiments in a competitive-cooperative process analogous to a tile puzzle (step 4) (Kohonen, 1998). As a result, metabolites that are produced as similar responses to the experimental conditions occupy the same or close coordinates in the grid. This sorts features in a data-driven manner into regions of correlated feature response (step 5).

The presumed correspondence of secondary metabolite expression profiles to responses is premised on the hypothesis that microorganisms use secondary metabolites to respond to discrete external stimuli (e.g., antibiotic challenge, competition, and metal exposure). The metabolic profile of each sample or experimental condition is then depicted as a topological heat map, which is a function of the intensity of each ion in that sample (step 6). Features occupying the same coordinates in the SOM are summed. These heat maps (cf. Figure 3), or metabolic profiles, are then differentially compared with unperturbed metabolic profiles, resulting in heat maps with prioritized ROIs, indicating metabolic responses to experimental conditions (step 7). Each pixel or node within the heat maps contains *m/z* R_t feature lists, which are used for subsequent feature identifications. We selected six ROIs based on visual comparison of the differential phenotype heat maps, generated tables of co-varying features via summing islands of high intensity within the heat maps, and ranked features by percentage (for more details, see the Supplemental Information). The species occupying these ROIs are then prioritized for further identification using accurate mass and fragmentation data acquired using MS^E technology. A given ROI may comprise only one or several species. To ascertain rank within a given ROI, percent contributions of each species to the total ROI intensity may be determined (see Supplemental Information). Through self-organization, features corresponding to fragment ions, adducts, and isotopes are also all clustered for rapid triage. Determination of the molecular identity of features is facilitated by untargeted fragmentation acquisition, accurate mass measurements, retention time, ion mobility drift time, and other fragmentation interpretation afforded by the ion mobility separation dimension, as described in Figure S2.

Figure 3 demonstrates the utility of the SOM-based approach for molecular prioritization using this workflow across the multiplexed inducing conditions reported for enhanced secondary

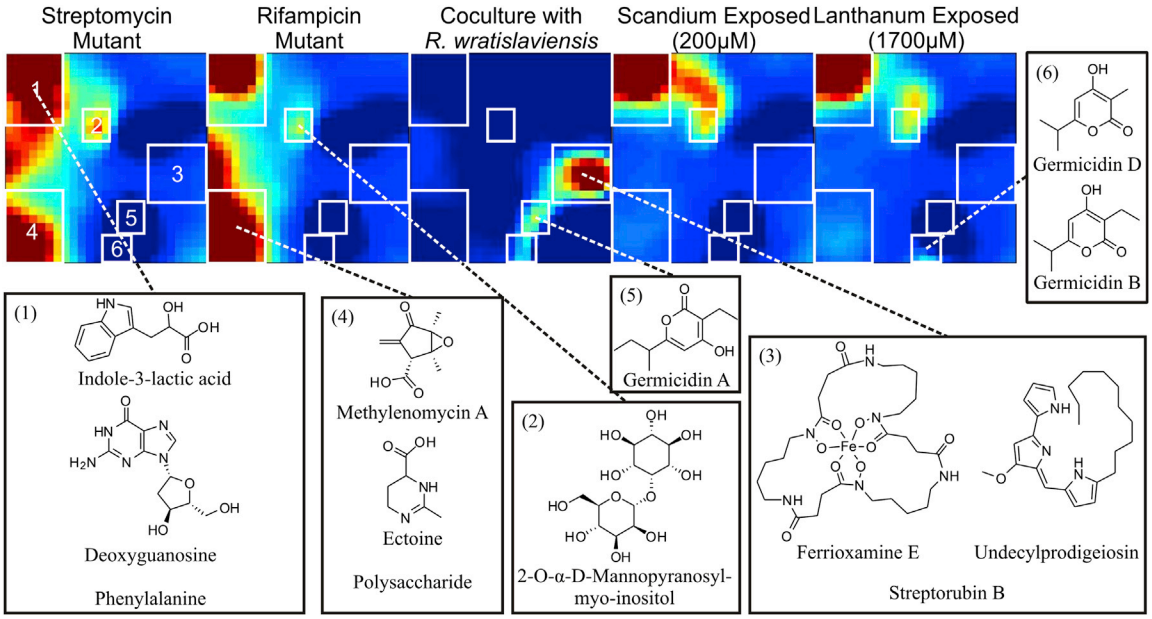

Figure 3. Differential Metabolic Phenotype Heat Maps Representing Increased Production/Decreased Consumption of Molecules Using a Single Growth Medium

Representative extracts from each culturing condition are shown above, with regions of interest (ROIs) boxed and labeled. Corresponding putative identifications and structures for each ROI are labeled, and comprehensive catalogs of inhabiting features for each region, including relative abundance and percent contribution to total ROI intensity, are presented in the Supplemental Information.

metabolite production. For heat maps of all tested conditions, please refer to Figure S3. Each heat map is representative of 2,154 detected features (including detected isotopologs) observed in *S. coelicolor* grown with a unique perturbation or condition, following subtraction of the unperturbed culture extract. In the case of monoclonal cultures (i.e., streptomycin- and rifampicin-selected point mutations, rare element exposure), this baseline subtraction is simply subtraction of the ISP2 unperturbed culture metabolic profile. In co-culturing conditions, metabolic profiles from both wild-type *S. coelicolor* and competing organism monoculture were subtracted, resulting in a map of feature inventories that are produced at increased levels in each mixed culture in comparison with the constituent monocultures. Hence, caveats in interpreting mixed culture data are that increased feature production can be a result of either organism, and the output of the mixed culture is likely more than the sum of its parts. Six dominant ROIs are indicated as boxed regions in Figure 3 and identified ions that occupy these regions are annotated (for a full list of all features occupying these regions, see the Supplemental Information, Tables S2 and S3). A majority of the annotated ions corresponds to secondary metabolites that *S. coelicolor* is known to produce (Challis, 2013). However, we gain additional biological insight into the microbial response to the various stimuli by observing the other biochemical results that are sorted with these secondary metabolites (e.g., deoxyguanosine, phenylalanine).

Measuring and Structuring Metabolic Perturbations

Each inducing condition provoked unique metabolic responses, as observed in the differential profiles in Figure 3. In total, of the 2,154 significant features detected, 1,318 were found to be either previously undetected or produced in at least 2-fold abundance in at least one perturbed system relative to control (see the Supplemental Information). This corresponds to induced overproduction of ~61% of all detected species. For the subset of known secondary metabolites, 16 were observed in at least one *S. coelicolor* expression condition (<20 ppm mass accuracy), including monoclonal culturing in liquid culture or agar. Molecular ions, corresponding mass accuracies, and comparative relative intensities appear in the Supplemental Information (Table S4; Figure S4). We found increased production of each of the 16 detected metabolites in at least one perturbed culture compared with the matched unperturbed control. The magnitude of amplification is shown in Figure 4. In certain cases, a nearly 22-fold increase in production was found (i.e., undecylprodigiosin).

Response Profile Analysis

Secondary metabolic gene clusters in microorganisms are often organized into operons, and within a given organism, gene clusters share common regulatory elements programmed to respond to specific cellular states (e.g., pleiotropic signals) (Bibb, 2005). Correspondingly, we hypothesize that secondary metabolite features that are differentially produced as a result of multiplexed chemical and biological stimuli will structure into grouped regions in a SOM of metabolites based on similarity of production response profiles. Herein, we describe and demonstrate the application of this approach, which ameliorates the limitations of MVSA-based analytics for multiplexed stimuli data interpretation. One practical advantage of the SOM approach is that dozens of chemical, biochemical, or genetic perturbations may be analyzed using a single computation (in

Metabolite[a]	Heavy Metals	Antibiotic Resistance	Co-culture
Undecylprodigiosin	98%	470%	2200%
Germidicidin A	120%	180%	130%
Germicidin B	140%	250%	140%
Germicidin D	250%	480%	84%
Methylenomycin A	110%	170%	98%
N-Acetylhistidinol	130%	220%	18%
Juglomycin D	160%	200%	20%
2-O-α-D-Mannopyranosyl -myo-inositol	300%	200%	62%
Streptorubin B	250%	110%	1300%
Coelichelin	100%	150%	16%
γ-Actinorhodin	170%	500%	29%
ε-Actinorhodin	100%	120%	61%
Antibiotic CDA 4A	130%	330%	87%
Ferrioxamine E	50%	150%	120%
Desferrioxamine B	280%	130%	220%
Indole-3-lactic acid	4600%	3400%	84%
Ectoine	250%	290%	240%

Figure 4. Maximum Resultant Metabolite Production Abundances Compared with Matched Control Cultures in ISP2 Medium

Color scale: 0% (red); 100% (yellow); 200% (green). Heavy metal and antibiotic resistance performed in liquid cultures and co-culture performed on agar medium. [a]Putative metabolite identification of metabolites reported to be produced by *S. coelicolor* based on accurate mass measurement and fragmentation pattern, when available.

this case 25 × 3 analyses, comprising >780,000 spectra, in excess of 58 gigabytes of data, spanning three classes of stimuli), resulting in the generation of sets of simple and easily navigable metabolic phenotype graphical representations that still retain the attributes of MVSA-based analytics. In addition, although features within an ROI can be ranked by abundance, SOM organizes features by intensity trends, so low-intensity features can also be identified even in the presence of large datasets.

At least 22 gene clusters within the *S. coelicolor* genome have been assigned involvement in secondary metabolite production (Bentley et al., 2002). Of these 22 clusters, SOM maps prioritized metabolites associated with 8 of the 22 gene clusters, which are listed in Table S1, of which all display elevated secondary metabolite production in some capacity as a result of the introduction of challenges (Figure 4). Putative metabolite feature intensity trends are shown in Table S2. In all cases, feature intensity profiles map consistently to the ROI. In some cases, however, putative features show false-positive intensity values due to coincident features of similar mass/retention time. For instance, actinorhodins and desferrioxamines are not produced by the challenge organisms, although features with a similar accurate mass were found. For a full table of relative abundances across all conditions, we direct the reader to Table S3. The analytical strategy presented prioritizes secondary metabolites generated from these gene clusters from within the metabolomic pool, yet this begs the question as to the biological rationale of these lower abundance, yet overproduced, species. Significantly, an increase in the production of germicidins (Figure 3, ROIs 5 and 6) was observed in both mixed fermentation conditions and selected antibiotic-resistant strains. Metabolomic analysis indicated that the process of culturing *S. coelicolor* on agar versus the liquid cultures affected the production of germicidins. However, germicidins A and B were present in higher concentrations in the mixed fermentation cultures versus the monoclonal cultures grown on agar, in addition to all germicidins observed in increased abundances in many of the antibiotic-resistant cultures. The production of germicidins inhibits spore germination and is a self-regulatory mechanism in the production response to high population densities (Aoki et al., 2011). In addition, mixed fermentation resulted in the enhanced production of undecylprodigiosin (22-fold increase when co-cultured) and streptorubin B (13-fold increase when co-cultured) (Figure 3, ROI 3), known secondary metabolites of *S. coelicolor* with antimicrobial and other clinically relevant properties (Williamson et al., 2006). This is consistent with previous studies that linked undecylprodigiosin and streptorubin B production to external factors, including mixed fermentation with *Bacillus subtilis* (Luti and Mavituna, 2011) and salt stress (Sevcikova and Kormanec, 2004). Within this same ROI, we observe the enhanced production of siderophores functioning as an iron scavenger for nutrient acquisition in all perturbed conditions (Barona-Gomez et al., 2006). This response is likely a concerted rebuttal to the microbial competition encountered in the mixed fermentation environment. A variant of calcium-dependent antibiotic production was observed to be upregulated (3.3-fold increase) specifically in agar culturing and co-culturing conditions with *T. pulmonis* (Figure S4). This Gram-positive targeting metabolite may be attributed to *T. pulmonis* production of mycolic acid, which activates secondary metabolite production in once silent clusters (Onaka et al., 2011) and underpins the necessity of multi-conditional culturing. We also observed altered production of potentially exo-polysaccharides (Figure 3, ROI 4) as a result of these persistent resistant mutations.

Furthermore, 2-*O*-α-D-mannopyranosyl-myo-inositol (3-fold increase in rare element exposure) was observed in increased abundance in mutant- and rare element-exposed cultures (Figure 3, ROI 2), the production of which has been demonstrated previously in liquid culture (Pospisil et al., 2007), supported by the absence in mixed fermentation conditions. Elevated production of ectoine (2.8-fold increase) was observed as a general response to perturbations and is consistent with previous results we have observed within rifampicin- and streptomycin-resistant mutants in *Nocardiopis* (Derewacz et al., 2013). This osmoprotectant has been shown to provide enzyme activity stabilizing effects (Lippert and Galinski, 1992) and stimulate growth in osmotically inhibitory environments (Jebbar et al., 1992).

DISCUSSION

Microbial genome sequencing has revealed a vast reservoir of secondary metabolite-encoding gene clusters, suggesting largely untapped molecular diversity with potential biomedical application. Advances in sequencing have outpaced the developments of the requisite steps to produce, study, and ultimately purify the encoded metabolites: gene cluster expression and translation, identification and purification of the resulting produced metabolites, and structure elucidation. Two complementary strategies for addressing the expression component of these processes consist of refactoring targeted gene clusters for increased expression, typically in heterologous hosts (Medema et al., 2011; Wilkinson and Micklefield, 2007; Yamanaka et al., 2014), or expression of gene clusters in their native hosts using nonrecombinant chemical or biochemical methods to stimulate native expression (Walsh and Fischbach, 2010; Zerikly and Challis, 2009), or via systematic modification of cultivation

parameters, also called OSMAC (One Strain-Many Compounds) (Bode et al., 2002). In either case, the analysis of the resulting metabolomes for upregulated or otherwise perturbed metabolites potentially becomes the next rate-limiting step. Rapid unbiased identification and prioritization of newly produced metabolites is an essential prerequisite for what remain the most labor-intensive steps of secondary metabolite discovery: purification, isolation, and structure elucidation.

This study analyzes three categories of microbial stimulus (antibiotic-induced resistance, heavy metal exposure, and coculture) on a single metabolomic platform. To convert the microbial metabolomic responses from 23 distinct conditions spanning these three perturbations into navigable phenotypic maps, we develop and implement SOM analytics for multiplexed responses to microbial metabolomics. This approach localizes metabolomic features that co-vary across conditions into ROIs that can be used to identify metabolic features that are similarly regulated, or that respond similarly to challenge. Secondary metabolites are the end products of metabolic pathways, accumulate, and are slowly degraded. As a result, they are well suited for the application of SOM analytics that not only prioritize features but also illuminate trends in similarly responding metabolites. Previous studies of biological, biochemical, and chemical microbial challenge are consistent with the hypothesis that the upregulation of secondary metabolism may be an adaptive response to challenge stimuli (Derewacz et al., 2013; Ochi et al., 2014; Tanaka et al., 2009). Moreover, the current study confirms the recent analysis of metabolomic dynamics engendered by a cohort of interspecies interactions (Traxler et al., 2013) and analyzed by nanospray desorption electrospray ionization. These results provide additional support for the broad-reaching effects of chemical and biological stimulus and a new means for identification of important microbial response chemicals.

Strategies using topological clustering of metabolomic data are finding increasing application in secondary metabolite discovery. For example, a molecular network analysis tool has recently been developed and applied to aid in the organization of exometabolic inventory analysis and to prioritize secondary metabolite discovery (Nguyen et al., 2013; Traxler et al., 2013). Metabolite molecular network analysis uses numerical clustering of tandem mass spectra similarity as an organizing principle and provides a map based on chemical similarity. This method also permits simultaneous graphical visualization of structural relatedness networks for multiple stimuli conditions or organisms and is excellent for dereplication and prioritization by chemical structure. The SOM method described herein is distinct from this method in that the organizing principle is not structure (inferred from fragment data) but rather response trends across more than two dozen conditions. Indeed, because SOM ROIs can contain hundreds of correlating features, molecular network analysis can potentially be used as a method to prioritize responsive features identified by SOM analytics, underlining the complementary nature of these methods. Other comparative metabolomics methods, such as bubble plot visualization, provide a straightforward and easily interpretable tool for determining differences in metabolomic feature production, but are generally only applicable to binary comparison and do not render correlations in ion profiles across many experimental conditions (Patti et al., 2012a). However, meta-XCMS procedures may find significant utility in this type of secondary metabolite prioritization (Patti et al., 2012b). Some unique advantages of the SOM method described here are that it can analyze the response patterns of 25+ stimuli conditions simultaneously and secondary metabolites can be identified from response trends via simple subtractive analysis using the trained map template as an organizing principle.

As accumulating dead ends of metabolic pathways, secondary metabolites are ideal candidates for the application of SOM analytics; however, the utility of this approach extends beyond secondary metabolism. For instance, we have recently applied the SOM metabolomics to the analysis of mouse serum and used it to identify diagnostic features in mice addicted to cocaine, demonstrating the general utility of this method for both abundant and nonabundant comparative metabolomics (Goodwin et al., 2014). In addition, Kohonen's SOM analytics has been used to understand time-dependent metabolite changes in rice plants, identifying synchronously fluctuating metabolites (Sato et al., 2008). Importantly, as datasets incorporate ever-increasing amounts of data (e.g., time, perturbation, etc.) the corresponding ROIs provide correspondingly higher specificity.

From a genome mining perspective, we observed substantial metabolomic expansion of the biomolecular inventory of *S. coelicolor* grown in a single medium using multiplexed chemical and biochemical induction methods. Of the nearly 2,200 total detected molecular features, 61% were found to be either undetected in control cultures or produced in at least 2-fold greater amounts, relative to control, in at least one culture challenge. Indeed, using these methodologically simple and rapid nonrecombinant techniques, we have observed the increased production of all 16 of the secondary metabolites detected, comprising products of up to 8 of 22 annotated gene clusters in at least one unique culturing condition, and prioritizing eight natural products within ROIs. These results challenge the notion of silent gene clusters in native hosts and support the potential of systematic induction of native secondary metabolism as a method of accessing the hidden reservoirs of secondary metabolic diversity in microorganisms. Indeed, with a comparatively small set of stimuli, which can be generated and analyzed in less than a month, the majority of known secondary metabolism was activated. Future studies combining analysis of transcriptional and metabolomic covariance with stimuli offer the potential to target the activation of specifically regulated gene clusters with a rationally selected set of challenges. In this way, chemistry and biology may be rationally manipulated in the future to quickly elicit the expression of cryptic or silent gene clusters in cultivatable organisms or alternatively in the assessment of heterologously or endogenously refactored gene clusters in microorganisms.

SIGNIFICANCE

We hypothesize that the inventory of metabolic features resulting from a microorganism's exposure to multiple chemical and biological stimuli can be used to identify induced expression of secondary metabolites. Central to this approach is the premise that microbial secondary metabolites are produced to respond to environmental stimuli. It

follows that their production can be revealed by examining the patterns of metabolomic feature responses across multiple stimuli. This responsomics approach has been applied here to the well-characterized actinomycete *S. coelicolor*, revealing that production of the majority of secondary metabolites in this strain can be induced by simple stimuli and subsequently identified by comparative metabolomics analysis via self-organizing maps. Regions of interest within the response maps reveal those metabolites that are characteristically modulated by multiplexed stimuli and ranking these by abundance provides a means of prioritizing compounds for isolation studies. The advantages of self-organizing map analytics are that it ranks features via response profile, not by intensity, permitting the identification of low-intensity features contributing to a response phenotype, it carries out the comparison of large numbers of datasets (up to 25 in this study) in a single computation, and provides easy to navigate heat maps of metabolic response phenotypes. In addition to providing a work flow for the identification of secondary metabolites, the ability to inventory metabolites that are modulated consistently via multiplexed stimuli may be used to identify features relevant to microbial physiology, development, and chemical ecology.

EXPERIMENTAL PROCEDURES

Materials and Methods

All reagents were obtained from Sigma-Aldrich unless otherwise specified. *S. coelicolor A3(2)* was obtained from the John Innes Center, *T. pulmonis* from the American Type Culture Collection (ATCC 700081), and *R. wratislaviensis* was obtained via dilution plating from hypogean sediments.

Eliciting Antibiotic Resistance and Fermentations

To generate antibiotic-resistant mutants, the spore inoculum of *S. coelicolor* was uniformly spread on GYM (glucose 0.4%, yeast extract 0.4%, malt extract 1%, peptone 0.1%, sodium chloride 0.2%, agar 2%) agar plates containing streptomycin at one of two concentrations (100 μg/ml, 300 μg/ml) or rifampicin at either 200 μg/ml or 400 μg/ml (concentrations of antibiotics were chosen so they exceed the minimum inhibitory concentration for *S. coelicolor* on GYM medium). After 2 weeks of incubation at 30°C, the agar plates were inspected for the presence of resistant colonies, which were then aseptically transferred to antibiotic-free ISP2 (glucose 0.4%, yeast extract 0.4%, malt extract 1%, agar 2%) plates. Each *S. coelicolor* mutant was then inoculated to 20 ml of ISP2 liquid seed culture and incubated for 7 days, and from seed culture to 50 ml of liquid ISP2 fermentation culture for 7 days of incubation at 30°C. Progenitor *S. coelicolor* was incubated under the same conditions to generate the control culture.

Rare Earth Element Fermentations

For rare element additives, the spore suspension of *S. coelicolor* was inoculated on ISP2 agar plates for incubation at 30°C for 7 days, then inoculated from plates into 20 ml of liquid seed culture and from seed culture to 50 ml of liquid ISP2 production cultures containing various concentrations of scandium chloride (20 μM, 50 μM, 100 μM, 200 μM, 500 μM) or lanthanum chloride (1500 μM, 1700 μM, 1900 μM, 2100 μM, 2500 μM) for 7-day incubations at 30°C. To generate a control, *S. coelicolor* was incubated in 50 ml of additive-free ISP2 medium under the same conditions.

Extraction of Liquid Fermentations

Total culture metabolite extracts from liquid cultures were generated by adding 50 ml of methanol to each fermentation flask and shaking the flasks on a rotary shaker for 1 hr. Mycelia were then separated on a centrifuge and supernatants were dried in vacuo to yield crude extracts.

Co-culture

Co-culture plates were prepared by addition of 40 ml of sterile ISP2 medium to a one-well OmniTray plate. Cryogenic spore suspensions of *S. ceolicolor* were cultivated on agar plates (100 × 15 mm) containing 30 ml of ISP2 medium and incubated at 30°C until the production of spores occurred. The spores were removed from the surface of the plate using a sterile loop and suspended in 25 ml of ISP2 liquid medium at a concentration of approximately 10^8 spores/ml as determined via hemocytometer. This suspension was homogenized and decanted into a one-well plate as a reservoir. The pins of a 96-well replicator were submerged into the spore solution and applied to the surface of the solid support within the previously prepared one-well OmniTray plate without puncturing the surface (Figure S1). The plates were incubated for 24 hr at 30°C. Cryogenically stored *M. luteus* was inoculated into 5 ml of sterile ISP2 medium 8 hr prior to application to the co-culture plate. *R. wratislaviensis* stock was inoculated into 5 ml of sterile ISP2 medium 24 hr prior to application to the co-culture plate. Cryogenically stored *T. pulmonis* stock was inoculated into 5 ml of sterile heart infusion medium 24 hr prior to application to the co-culture plate. For all competing organisms, once an OD_{600} of ~1 was achieved, the 5-ml sample was diluted into 30 ml of medium in separate one-well plate reservoirs. The pins of a 96-well replicator were submerged into the solution and applied to the surface of the solid support within the one-well OmniTray plate without puncturing the surface in an offset manner relative to the previously inoculated actinomycete. After 7 days, co-cultures plates were cut into 1 × 1 cm segments and extracted with equal volumes of methanol by shaking for 3 hr at 170 rpm and 30°C.

UPLC-IM-MS Data Acquisition and Processing

Extract samples were resuspended in methanol at a concentration of 200 mg/ml. UPLC-IM-MS^E data acquisition was performed with a 25-min gradient. Mobile phase A consisted of H_2O with 0.1% formic acid and mobile phase B consisted of acetonitrile with 0.1% formic acid. A 1 × 100 mm 1.7-μm particle BEH-T3 C18 column (Waters) was used for chromatographic separations with a flow rate of 75 μl/min and a column temperature of 40°C. An autosampler with a loop size of 5 μl held at 4°C was used for sample injection. The initial solvent composition was 100% A, which was held for 1 min and ramped to 0% A over the next 11 min, held at 0% A for 2 min, and returned to 100% A over a 0.1-min period. The gradient was held at 100% A for the next 10.9 min for equilibration. Prior to analysis of the sample queue, ten sequential column-load injections were performed with 5 μl of the quality control. This protocol increases retention time stability and is critical to reproducible analyses. Quality control injections were then performed after every ten sample injections to ensure instrument stability. Quality controls comprised pooled equal aliquots of all samples analyzed.

IM-MS^E spectra were acquired at a rate of 2 Hz from 50 to 2000 Da in positive ion mode for the duration of each sample analysis on a Synapt G2 HDMS platform (Waters). The instrument was calibrated to less than 1 ppm mass accuracy using sodium formate clusters prior to analysis. A two-point internal standard of leucine enkephalin was infused in parallel to the sample at a flow rate of 7 μl/min and data were acquired every 10 s. The source capillary was held at 110°C and 3.0 kV, with a desolvation gas flow of 400 l/hr and a temperature of 150°C. The sampling cone was held at a setting of 35.0, with the extraction cone at a setting of 5.0. In the MS^E configuration, low and high energy spectra were acquired for each scan. High energy data provided a collision energy profile from 10 to 30 eV in the trapping region, providing post-mobility fragmentation. Ion mobility separations were performed with a wave velocity of 550 m/s, a wave height of 40.0 V, and a nitrogen gas flow of 90 ml/min, with the helium cell flow rate at 180 ml/min. Internal calibrant correction was performed in real time.

Data were converted to mzXML format using the msconvert tool from the ProteoWizard package (Kessner et al., 2008). Peak picking and alignment were performed using XCMS in R (Smith et al., 2006). See Figure S2 for details and package locations. The resulting data matrix contained 2,154 detected features and was formatted for analysis using both GEDI and Umetrics. Formatting for GEDI is outlined below; formatting for Umetrics was performed by extracting and transposing the sample-feature intensity matrix generated from XCMS and importing it into Umetrics software. Prior to GEDI and MVSA, analytical triplicates were averaged. For GEDI analysis, a grid of 25 × 26 was generated. Software-specific parameters include 100 first phase training iterations with an initial training radius of 10.0, a learning factor of 0.5, a neighborhood block size of 20, and a conscience of 5.0; and 160 second-phase training iterations with a neighborhood radius of 1.0, learning factor of 0.05, neighborhood block size of 2, and conscience of 2.0. A random seed

of 10 with a Pearson correlation distance metric and random selection initialization was used.

Metabolite identifications were performed using accurate mass measurements and fragmentation spectra extracted from IM-MS^E data. Utilizing drift time correlations, product ions were correlated appropriately to precursors for extraction of high energy spectra.

SUPPLEMENTAL INFORMATION

Supplemental Information includes Experimental Materials and Methods, four figures, and four tables and can be found with this article online at http://dx.doi.org/10.1016/j.chembiol.2015.03.020.

AUTHOR CONTRIBUTIONS

D.K.D. performed the heavy metal and antibiotic resistance culturing and extraction. C.R.M and B.C.C. performed the co-culturing and extraction. C.R.G. and R.C.M developed the mixed culture apparatus. C.R.G. performed the mass spectrometry acquisition and analytics. D.K.D, B.C.C, C.R.G., J.A.M., J.P.W., and B.O.B. wrote the manuscript.

ACKNOWLEDGMENTS

We acknowledge support from NIH grant 1R01GM92218, the Defense Threat Reduction Agency grant HDTRA1-09-1-0013, the Vanderbilt Institute of Chemical Biology, the Vanderbilt Institute for Integrative Biosystems Research and Education, Vanderbilt University, and the Systems Biology and Bioengineering Undergraduate Research Experience (SyBBURE) funded by Gideon Searle at Vanderbilt. We thank Dr. Carol A. Rouzer for her gracious and significant editorial and intellectual contributions and guidance. We also thank Ms. Allison Price for her editorial assistance.

Received: May 13, 2014
Revised: March 26, 2015
Accepted: March 30, 2015
Published: April 30, 2015

REFERENCES

Aoki, Y., Matsumoto, D., Kawaide, H., and Natsume, M. (2011). Physiological role of germicidins in spore germination and hyphal elongation in *Streptomyces coelicolor* A3(2). J. Antibiot. *64*, 607–611.

Barona-Gomez, F., Lautru, S., Francou, F.-X., Leblond, P., Pernodet, J.-L., and Challis, G.L. (2006). Multiple biosynthetic and uptake systems mediate siderophore-dependent iron acquisition in *Streptomyces coelicolor* A3(2) and *Streptomyces ambofaciens* ATCC 23877. Microbiology *152*, 3355–3366.

Bentley, S.D., Chater, K.F., Cerdeno-Tarraga, A.M., Challis, G.L., Thomson, N.R., James, K.D., Harris, D.E., Quail, M.A., Kieser, H., and Harper, D. (2002). Complete genome sequence of the model actinomycete *Streptomyces coelicolor* A3(2). Nature *417*, 141–147.

Bibb, M.J. (2005). Regulation of secondary metabolism in streptomycetes. Curr. Opin. Microbiol. *8*, 208–215.

Bode, H.B., Bethe, B., Hofs, R., and Zeeck, A. (2002). Big effects from small changes: possible ways to explore nature's chemical diversity. ChemBioChem *3*, 619–627.

Challis, G.L. (2013). Exploitation of the *Streptomyces coelicolor* A3(2) genome sequence for discovery of new natural products and biosynthetic pathways. J. Ind. Microbiol. Biotechnol. *41*, 219–232.

Craney, A., Ozimock, C., Pimentel-Iardo, S.M., and Nodwell, J.R. (2012). Chemical perturbation of secondary metabolism demonstrates important links to primary metabolism. Chem. Biol. *24*, 1020–1027.

Derewacz, D.K., Goodwin, C.R., McNees, C.R., McLean, J.A., and Bachmann, B.O. (2013). Antimicrobial drug resistance affects broad changes in metabolomic phenotype in addition to secondary metabolism. Proc. Natl. Acad. Sci. USA *110*, 2336–2341.

Eichler, G.S., Huang, S., and Ingber, D.E. (2003). Gene Expression Dynamics Inspector (GEDI): for integrative analysis of expression profiles. Bioinformatics *19*, 2321–2322.

Goodwin, C.R., Fenn, L.S., Derewacz, D.K., Bachmann, B.O., and McLean, J.A. (2012). Structural mass spectrometry: rapid methods for separation and analysis of peptide natural products. J. Nat. Prod. *75*, 48–53.

Goodwin, C.R., Sherrod, S.D., Marasco, C.C., Bachmann, B.O., Schramm, S.N., Wikswo, J.P., and McLean, J.A. (2014). Phenotypic mapping of metabolic profiles using self-organizing maps of high-dimensional mass spectrometry data. Anal. Chem. *86*, 6563–6571.

Hosaka, T., Ohnishi-Kameyama, M., Muramatsu, H., Murakami, K., Tsurumi, Y., Kodani, S., Yoshida, M., Fujie, A., and Ochi, K. (2009). Antibacterial discovery in actinomycetes strains with mutations in RNA polymerase or ribosomal protein S12. Nat. Biotechnol. *27*, 462–464.

Hou, Y., Braun, D.R., Michel, C.R., Klassen, J.L., Adnani, N., Wyche, T.P., and Bugni, T.S. (2012). Microbial strain prioritization using metabolomics tools for the discovery of natural products. Anal. Chem. *84*, 4277–4283.

Jebbar, M., Talibart, R., Gloux, K., Bernard, T., and Blanco, C. (1992). Osmoprotection of *Escherichia coli* by ectoine: uptake and accumulation characteristics. J. Bacteriol. *174*, 5027–5035.

Kessner, D., Chambers, M., Burke, R., Agus, D., and Mallick, P. (2008). ProteoWizard: open source software for rapid proteomics tools development. Bioinformatics *24*, 2534–2536.

Kohonen, T. (1998). Self-organization of very large document collections: state of the art. In Proceedings of ICANN98, the 8th International Conference on Artificial Neural Networks, L. Niklasson, M. Boden, and T. Ziemke, eds. (Springer), pp. 65–74.

Lippert, K., and Galinski, E. (1992). Enzyme stabilization by ectoine-type compatible solutes: protection against heating, freezing and drying. Appl. Microbiol. Biotechnol. *37*, 61–65.

Luti, K., and Mavituna, F. (2011). *Streptomyces coelicolor* increases the production of undecylprodigiosin when interacted with *Bacillus subtilis*. Biotechnol. Lett. *33*, 113–118.

McLean, J. (2009). The mass-mobility correlation redux: the conformational landscape of anhydrous biomolecules. J. Am. Soc. Mass Spectrom. *20*, 1775–1781.

Medema, M.H., Breitling, R., Bovenberg, R., and Takano, E. (2011). Exploiting plug-and-play synthetic biology for drug discovery and production in microorganisms. Nat. Rev. *9*, 131–137.

Moree, W.J., Phelan, V.V., Wu, C.H., Bandeira, N., Cornett, D.S., Duggan, B.M., and Dorrestein, P.C. (2012). Interkingdom metabolic transformations captured by microbial imaging mass spectrometry. Proc. Natl. Acad. Sci. USA *109*, 13811–13816.

Nguyen, D.D., Wu, C.-H., Moree, W.J., Lamsa, A., Medema, M.H., Zhao, X., Gavilan, R.G., Aparicio, M., Atencio, L., Jackson, C., et al. (2013). MS/MS networking guided analysis of molecule and gene cluster families. Proc. Natl. Acad. Sci. USA *110*, E2611–E2620.

Ochi, K., Tanaka, Y., and Tojo, S. (2014). Activating the expression of bacterial cryptic genes by rpoB mutations in RNA polymerase or by rare earth elements. J. Ind. Microbiol. Biotechnol. *41*, 403–414.

Onaka, H., Mori, Y., Igarashi, Y., and Furumai, T. (2011). Mycolic acid-containing bacteria induce natural-product biosynthesis in *Streptomyces* species. Appl. Environ. Microbiol. *77*, 400–406.

Patti, G.J., Tautenhahn, R., Rinehart, D., Cho, K., Shriver, L.P., Manchester, M., Nikolskiy, I., Johnson, C.H., Mahieu, N.G., and Siuzdak, G. (2012a). A view from above: cloud plots to visualize global metabolomic data. Anal. Chem. *85*, 798–804.

Patti, G.J., Tautenhahn, R., and Siuzdak, G. (2012b). Meta-analysis of untargeted metabolomic data from multiple profiling experiments. Nat. Protoc. *7*, 508–516.

Plumb, R.S., Johnson, K.A., Rainville, P., Smith, B.W., Wilson, I.D., Castro-Perez, J.M., and Nicholson, J.K. (2006). UPLC/MSE; a new approach for generating molecular fragment information for biomarker structure elucidation. Rapid Commun. Mass Spectrom. *20*, 1989–1994.

Pospisil, S., Sedmera, P., Halada, P., and Petricek, M. (2007). Extracellular carbohydrate metabolites from *Streptomyces coelicolor* A3(2). J. Nat. Prod. *70*, 768–771.

Robinette, S.L., Bruschweiler, R., Schroeder, F.C., and Edison, A.S. (2012). NMR in metabolomics and natural products research: two sides of the same coin. Acc. Chem. Res. *45*, 288–297.

Sato, S., Arita, M., Soga, T., Nishioka, T., and Tomita, M. (2008). Time-resolved metabolomics reveals metabolic modulation in rice foliage. BMC Syst. Biol. *2*, 51.

Sevcikova, B., and Kormanec, J. (2004). Differential production of two antibiotics of *Streptomyces coelicolor* A3(2), actinorhodin and undecylprodigiosin, upon salt stress conditions. Arch. Microbiol. *181*, 384–389.

Seyedsayamdost, M.R. (2014). High-throughput platform for the discovery of elicitors of silent bacterial gene clusters. Proc. Natl. Acad. Sci. USA *111*, 7266–7271.

Smith, C.A., Elizabeth, J., O'Maille, G., Abagyan, R., and Siuzdak, G. (2006). XCMS: processing mass spectrometry data for metabolite profiling using nonlinear peak alignment, matching, and identification. Anal. Chem. *78*, 779–787.

Song, L., Barona-Gomez, F., Corre, C., Xiang, L., Udwary, D.W., Austin, M.B., Noel, J.P., Moore, B.S., and Challis, G.L. (2006). Type III polyketide synthase B-ketoacyl-ACP starter unit and ethylmalonyl-CoA extender unit selectivity discovered by *Streptomyces coelicolor* genome mining. J. Am. Chem. Soc. *128*, 14754–14755.

Tanaka, Y., Komatsu, M., Okamoto, S., Tokuyama, S., Kaji, A., Ikeda, H., and Ochi, K. (2009). Antibiotic overproduction by rpsL and rsmG mutants of various actinomycetes. Appl. Environ. Microbiol. *75*, 4919–4922.

Tanaka, Y., Hosaka, T., and Ochi, K. (2010). Rare earth elements activate the secondary metabolite biosynthetic gene clusters in *Streptomyces coelicolor* A3(2). J. Antibiot. *63*, 477–481.

Tanaka, Y., Kasahara, K., Hirose, Y., Murakami, K., Kugimiya, R., and Ochi, K. (2013). Activation and products of the cryptic secondary metabolite biosynthetic gene clusters by rifampicin resistance (rpoB) mutations in actinomycetes. J. Bacteriol. *195*, 2959–2970.

Traxler, M.F., Watrous, J.D., Alexandrov, T., Dorrestein, P.C., and Kolter, R. (2013). Interspecies interactions stimulate diversification of the *Streptomyces coelicolor* secreted metabolome. MBio *4*, e00459-13.

Walsh, C.T., and Fischbach, M.A. (2010). Natural products version 2.0: connecting genes to molecules. J. Am. Chem. Soc. *132*, 2469–2493.

Wilkinson, B., and Micklefield, J. (2007). Mining and engineering natural-product biosynthetic pathways. Nat. Chem. Biol. *3*, 379–386.

Williamson, N.R., Fineran, P.C., Leeper, F.J., and Salmond, G.P.C. (2006). The biosynthesis and regulation of bacterial prodiginines. Nat. Rev. *4*, 887–899.

Xu, J., Tozawa, Y., Lai, C., Hayashi, H., and Ochi, K. (2002). A rifampicin resistance mutation in the rpoB gene confers ppGpp-independent antibiotic production in *Streptomyces coelicolor* A3(2). Mol. Genet. Genomics *268*, 179–189.

Yamanaka, K., Reynolds, K.A., Kersten, R.D., Ryan, K.S., Gonzalez, D.J., Nizet, V., Dorrestein, P.C., and Moore, B.S. (2014). Direct cloning and refactoring of a silent lipopeptide biosynthetic gene cluster yields the antibiotic taromycin A. Proc. Natl. Acad. Sci. USA *111*, 1957–1962.

Zerikly, M., and Challis, G.L. (2009). Strategies for the discovery of new natural products by genome mining. ChemBioChem *10*, 625–633.

